JOURNAL OF APPLIED ELECTROCHEMISTRY **24** (1994) 772–778

Impedance spectroscopic study of aluminium and Al-alloys in acid solution: inhibitory action of nitrogen containing compounds

M. METIKOŠ-HUKOVIĆ, R. BABIĆ

Department of Electrochemistry, Faculty of Chemical Engineering and Technology, University of Zagreb, Savska c. 16/I, 41000 Zagreb, Croatia

Z. GRUBAČ, S. BRINIĆ

Department of Inorganic Chemistry, Faculty of Technology, University of Split, N. Tesle 10, 58000 Split, Croatia

Received 26 July 1993; revised 15 November 1993

The adsorption behaviour of triethanolamine (TEA) on aluminium, AlMgSi and AlZnMg alloys covered with naturally formed oxide films was investigated in 0.5 M NaCl solution, pH 1.3, by means of potentiodynamic and electrochemical impedance spectroscopy techniques. The results of polarization measurements show that in all cases the addition of TEA induces a decrease in the cathodic currents without affecting the anodic polarization behaviour, and, accordingly, TEA can be treated as a cathodic type inhibitor. The adsorption behaviour of TEA on the electrode surface follows a Frumkin isotherm with constants: $a = 1.74$, $B = 18.41\ \mathrm{dm^3\ mol^{-1}}$. The results of impedance measurements presented in Nyquist plots show a high frequency capacitive loop related to the dielectric properties of the oxide film and a low-frequency inductive part which was determined by the faradaic process and attributed to the localized corrosion.

List of symbols

a	attraction constant
B	constant of adsorption equilibrium ($\mathrm{dm^3\ mol^{-1}}$)
b	Tafel slope (mV)
C	capacity ($\mu\mathrm{F\ cm^{-2}}$)
CPE	constant phase element
c	concentration, $\mathrm{mol\ dm^{-3}}$
d	thickness (m)
E	potential (mV)
f	frequency (Hz)
j	current density ($\mathrm{mA\ cm^{-2}}$)
L	inductance ($\mathrm{Hy\ cm^2}$)
R	resistance ($\Omega\ \mathrm{cm^2}$)
$s = \mathrm{j}\omega$	complex variable for sinusoidal perturbations with $\omega = 2\pi f$
Z	impedance ($\Omega\ \mathrm{cm^2}$)
x	size ratio

Greek letters

θ	surface coverage (%)
ν	scan rate ($\mathrm{mV\ s^{-1}}$)
ω	angular speed ($\mathrm{rad\ s^{-1}}$)
ϵ_0	vacuum permittivity ($8.85 \times 10^{-12}\ \mathrm{F\ m^{-1}}$)
ϵ	dielectric constant

Sub/superscripts

a	anodic
b	cathodic
corr	corrosion
i	inhibition
el	electrolyte
p	polarization
pit	pitting
ct	charge transfer

1. Introduction

Aluminium has high resistance to corrosion in many environments; this is attributable to a protective surface film formed rapidly in air or in neutral aqueous solutions, and which is preserved even after long periods of immersion in acidic and alkaline media [1]. In recent years new data have been obtained on the electrochemical behaviour of aluminium in different aqueous solutions, particularly regarding either the role played by the oxide layer [2–5], or pitting corrosion due to the presence of chloride ions [5–11]. Corrosion of aluminium may occur through the oxide film by ionic migration followed by dissolution at the oxide/electrolyte interface. In pitting there is evidence of a salt film formation within the pits through which corrosion occurs [7]. Even in highly acidic solutions, such as hydrochloric acid, the oxide film has to be taken into account [6].

Generally, local corrosion attack can be prevented by [12]: (i) the action of adsorptive inhibitors which prevent the adsorption of the aggressive anions, and (ii) the formation of a more resistant oxide film on the metallic surface.

0021-891X

A number of organic compounds are described as aluminium corrosion inhibitors in acidic media [13–16]. As a rule, the same compounds used to protect iron and steel in hydrochloric acid can be used also to inhibit corrosion of aluminium and aluminium alloys, but with less efficiency [13]. Recent developments concerning the adsorption of organic compounds at electrodes are critically examined and discussed by Trabanelli [17] and Trasatti [18]. The study of the adsorption of organic substances at electrodes has attracted a wide interest because of its impact on our understanding, not only the inhibition of corrosion [19, 20], but also the structure of the electrical double layer, the kinetics of electron transfer and the role of intermediates in the mechanism of electrode processes [18].

The present study tests the influence of triethanolamine (TEA) on the corrosion of aluminium and its alloys covered with naturally formed oxide film in acidic medium, by means of potentiodynamic measurements and electrochemical impedance spectroscopy (EIS). The latter is a powerful technique for the study of electrochemical systems, including corrosion, and has found wide application in the study of corrosion phenomena on aluminium and its alloys in aggressive media [2–5, 11, 21–26]. For these studies it is important to develop appropriate models for the impedance, which can then be used to fit the experimental data and extract the parameters which characterize the corrosion process.

2. Experimental details

The samples selected for study had the following composition (in weight per cent): Al, 99.5: Cu, 0.01; Si, 0.01; Fe, 0.27; Ti, 0.01. AlMgSi: Cu, 0.01; Mn, 0.05; Mg, 0.09; Si, 0.46; Fe, 0.29; Ti, 0.015. AlZnMg: Cu, 0.02; Mn, 0.44; Mg, 1.29; Si, 0.20; Fe, 0.36; Zn, 4.69; Ti, 0.010.

Disc electrodes suitable for the EG&G PARC Model 616 system were machined from cylindrical rods of diameter 8 mm. The electrode surface was abraded with emery paper to an 800 metallographic finish, degreased in trichloroethylene and rinsed with triply distilled water. Prior to each electrochemical experiment, the electrode was left for 30 min in air. In all measurements the counter electrode was a platinum gauze and the reference electrode was a saturated calomel electrode (SCE). All potentials are referred to the SCE.

Measurements were performed in a 0.5 M NaCl solution, pH 1.3, (adjusted by a concentrated HCl solution), and in the presence of the inhibitor. After addition of TEA, which is a weak base, the initial pH value was restored by addition of the requisite amounts of concentrated HCl. All solutions were deaerated by argon.

Measurements were carried out in a standard electrochemical cell with a separate compartment for the reference electrode, connected with the main compartment via a Luggin capillary. The cell was a water-jacketed version, connected to a constant temperature circulator at 25° C.

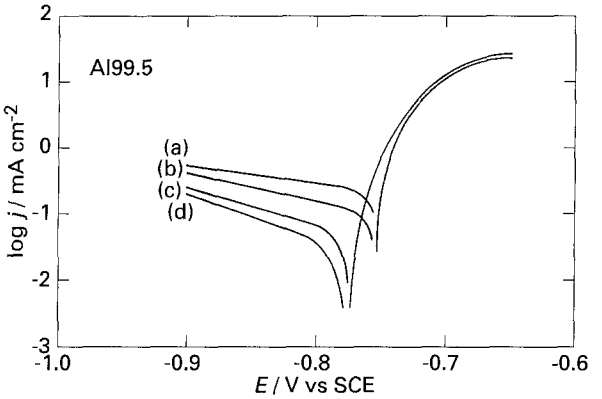

Fig. 1. Tafel plots obtained for an aluminium electrode in 0.5 M NaCl solution, pH 1.3 without (a) and in the presence of triethanolamine: (b) 0.010, (c) 0.015 and (d) 0.02 M; $n = 2000\,\mathrm{min}^{-1}$, $\nu = 2\,\mathrm{mV\,s}^{-1}$.

The polarization E against I curves were obtained by means of the linear potential sweep technique with a sweep rate of $2\,\mathrm{mV\,s}^{-1}$, and with a selected rotation rate of $2000\,\mathrm{min}^{-1}$, above which the shape of the polarization curves remained unchanged. Impedance measurements were performed in still conditions in the frequency range 30 mHz to 100 kHz; the a.c. voltage amplitude was ± 5 mV. All measurements were performed using a PAR potentiostat, Model 273A and a PAR lock-in amplifier, model 5301A with an IBM PS/2 computer.

3. Results and discussion

3.1. *Polarization measurements*

Figure 1 represents the potentiodynamic polarization curves obtained on aluminium in a 0.5 M NaCl solution, pH 1.3 with and without addition of TEA in different concentrations. Because the anodic currents corresponding to different inhibitor concentrations were close to each other, only the currents obtained in 0.5 M NaCl solution, pH 1.3, and in the presence of 0.02 M TEA are presented in Fig. 1. The increase in inhibitor concentration shifts E_{corr} cathodically, lowers the cathodic current densities with simultaneous

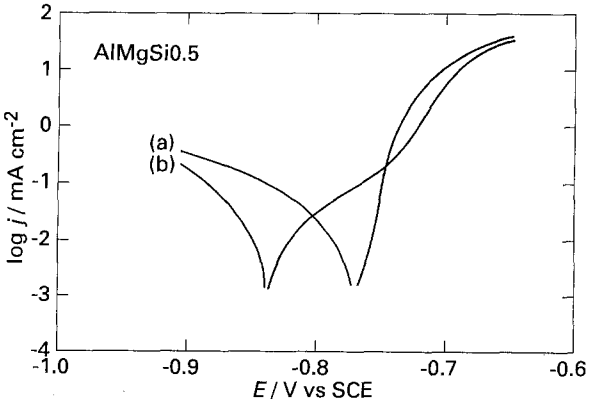

Fig. 2. Tafel plots obtained for an AlMgSi electrode in 0.5 M NaCl solution, pH 1.3 without (a) and in the presence of 0.02 M triethanolamine (b); $n = 2000\,\mathrm{min}^{-1}$, $\nu = 2\,\mathrm{mV\,s}^{-1}$.

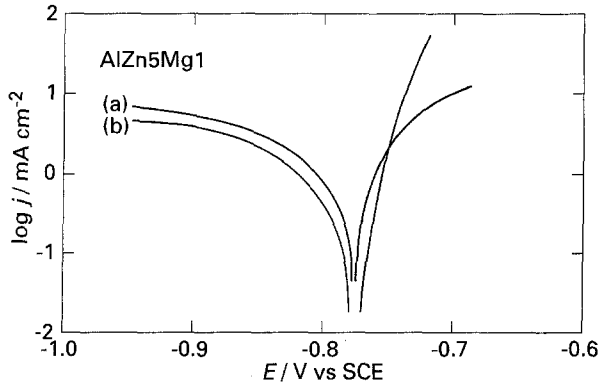

Fig. 3. Tafel plots obtained for an AlZnMg electrode in 0.5 M NaCl solution, pH 1.3 without (a) and in the presence of 0.02 M triethanolamine (b); $n = 2000\,\text{min}^{-1}$, $\nu = 2\,\text{mV s}^{-1}$.

decrease in Tafel b_c value and has almost no influence on the anodic current densities above approximately −0.72 V.

Figure 2 represents the potentiodynamic polarization curves obtained on AlMgSi alloy in a 0.5 M NaCl solution, pH 1.3, and in the presence of inhibitor (0.02 M). As in the previous case, the addition of inhibitor in a 0.5 M NaCl solution shifts E_{corr} cathodically, lowers the cathodic current densities with simultaneous decrease in Tafel b_c slope and has little influence on the anodic currents above about −0.7 V. It is interesting to note that the anodic current shows an intermediate plateau in the potential range between E_{corr} and −0.7 V, which is better expressed in the presence of inhibitor.

Figure 3 represents the potentiodynamic polarization curves obtained on AlZnMg alloy in 0.5 M NaCl solution, pH 1.3, and in the presence of inhibitor (0.02 M). The addition of inhibitor in a 0.5 M NaCl solution does not shift E_{corr}, but lowers the cathodic current densities. The anodic current densities above −0.8 V are larger in the presence of inhibitor than in a 0.5 M NaCl solution.

Electrochemical parameters E_{corr} and cathodic Tafel slopes determined from the polarization curves in Figs 1–3 are listed in Table 1. The values of corrosion currents determined by the extrapolation of cathodic Tafel curves to E_{corr} are also presented in Table 1 together with the inhibition efficiency (i.e. the surface coverage), θ, which was calculated using the equation: $\theta = [1 - (j_{corr})_i/(j_{corr})_0]100$, where $(j_{corr})_0$ and $(j_{corr})_i$ are the current densities without and in the presence of inhibitor.

The polarization measurements show, in all cases, that the addition of the inhibitor induces a decrease in the cathodic currents without affecting the anodic polarization behaviour, and, accordingly, TEA is a cathodic type inhibitor. The observed shift of E_{corr} on Al and AlMgSi alloy in the presence of inhibitor indicates that TEA inhibits the localized attack on these surfaces, since the difference $\Delta E = E_{pit} - E_{corr}$ appears to be a proper parameter to rate the inhibiting efficiency of the substances against localized corrosion [27]. Such an E_{corr} shift was not observed on AlZnMg alloy.

Before proceeding with a development of equations describing the mechanism of adsorption occurring at the electrolyte–oxide interface, a particular model for these processes is required. The following model will be assumed and is consistent with that arising from studies of the double layer at oxide–solution interfaces [28]. Equilibrium is assumed with respect to reactions of the following type:

$$\left(\begin{matrix}\succ\text{Al–OH}\\ \\ \succ\text{Al–OH}\end{matrix}\right)_{\text{surface}} \rightleftharpoons \left(\begin{matrix}\succ\text{Al}\\ \diagdown\ \diagup\ \text{O}\\ \succ\text{Al}\end{matrix}\right)_{\text{surface}} + \text{H}_2\text{O} \quad (1)$$

TEA molecules have electron-donating ability and can displace adsorbed water on the surface [29, 30] by hydrogen, bridging with its unshared electron pair as follows:

$$\begin{aligned}&\text{Al}:\underset{\text{H}}{\text{O}}\text{–H} + :\text{N}(\text{CH}_2\text{CH}_2\text{OH})_3\\ &\longrightarrow \text{Al}:\underset{\text{H}}{\text{O}}\text{–H}\ldots\text{N}(\text{CH}_2\text{CH}_2\text{OH})_3\\ &\longrightarrow \text{Al} + \underset{\text{H}}{\text{O}}\text{–H}\ldots\text{N}(\text{CH}_2\text{CH}_2\text{OH})_3 \quad (2)\end{aligned}$$

Table 1. Electrochemical parameters and inhibition efficiencies for Al, AlMgSi and AlZnMg alloys in a 0.5 M NaCl solution, pH 1.3

Sample	*C(TEA)* /mol dm^{-3}	$-E_{corr}$ /mV	j_{corr} /μA cm^2	b_c /mV	R_p /Ω cm^2	θ %
Al 99.5	nil	751	304	446	345	–
	1×10^{-3}	750	290	430	350	4.60
	5×10^{-3}	747	260	329	397	14.57
	10×10^{-3}	750	200	185	512	34.21
	15×10^{-3}	767	68	180	598	77.63
	20×10^{-3}	774	26	150	620	91.45
AlMgSi	nil	759	24	112	537	–
	20×10^{-3}	831	13	105	694	45.83
AlMg	20×10^{-3}	810	1320	224	24	29.22
	nil	817	1865	216	25	–

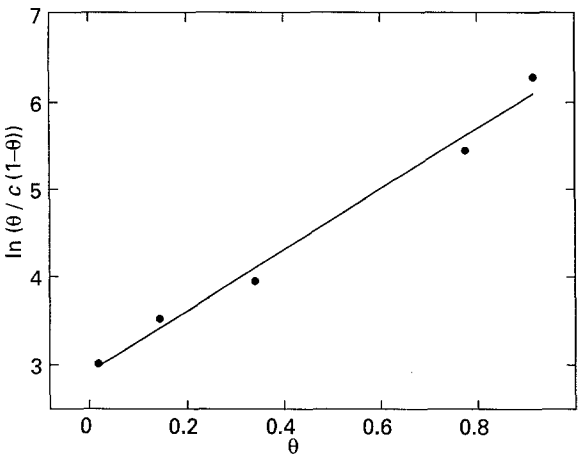

Fig. 4. Frumkin's adsorption isotherm on an aluminium electrode in a solution of triethanolamine in 0.5 M NaCl at pH 1.3. $a = 1.74$, $B = 18.41\ \mathrm{dm^3\ mol^{-1}}$, $r = 0.99338$.

After losing adsorbed water the electrode surface becomes electron-acceptable, and inhibitor molecules can be easily adsorbed:

$$\mathrm{Al} + : \mathrm{N(CH_2CH_2OH)_3} \longrightarrow \mathrm{Al} : \mathrm{N(CH_2CH_2OH)_3} \qquad (3)$$

The validity of Frumkin's adsorption isotherm which describes the adsorption of many organic compounds on the electrodes [31] was checked. The linear logarithmic form was used:

$$\ln \theta/c(1-\theta) = \ln B + 2a\theta \qquad (4)$$

where B is the constant of the adsorption equilibrium including the adsorption energy, and a is the attraction constant characterizing the lateral interaction between the molecules in the adsorption layer.

Figure 4 presents the dependence of $\ln \theta/c\,(1-\theta)$ against θ. The straight line is drawn using the least-squares method with the correlation coefficient 0.99, which suggests that the experimental data are well described by Frumkin's adsorption isotherm. The slope of the straight line gives the value 1.74 for the attraction constant. From the intercept of the straight line dependence for $\theta = 0$ the constant B, which is a criterion for the interaction between the adsorbed molecules and the surface, is estimated as $18.41\ \mathrm{dm^3\ mol^{-1}}$.

The adsorption of an organic adsorbate on the surface of a metal is regarded as a substitutional adsorption process between the organic compound in the aqueous phase $\mathrm{Org_{(aq)}}$ and the water molecules adsorbed on the electrode surface $\mathrm{H_2O_{(s)}}$ [32]:

$$\mathrm{Org_{(aq)}} + x\mathrm{H_2O_{(s)}} \rightleftharpoons \mathrm{Org_{(s)}} + x\mathrm{H_2O} \qquad (5)$$

where x is the size ratio, which is the number of water molecules replaced by one molecule of organic adsorbate. Expression 4 is only valid when one adsorbed molecule displaces one $\mathrm{H_2O}$ molecule from the surface ($x = 1$).

3.2. *Electrochemical impedance spectroscopy measurements*

Impedance measurements on aluminium and aluminium alloys performed at the open circuit potential 30 min after the electrodes had been immersed in electrolyte solution are represented in the form of Nyquist and Bode plots in Fig. 5(a) and (b).

In the Nyquist plot all three samples show a high frequency capacitive loop together with a low frequency inductive loop. The high frequency capacitive loop can be correlated with the dielectric properties of the oxide film, while the low-frequency inductive loop of the impedance can be attributed to the observed localized process.

In the Bode plot the high frequency limit corresponds to the electrolyte resistance R_{el}. The low frequency limit represents the sum of R_{el} and the resistance R_p, which is in the first approximation determined by both the electronic conductivity of the oxide film and the polarization resistance of the dissolution and repassivation processes. The phase angle, θ, against $\log f$ plot shows θ dropping towards zero at high and low frequencies, corresponding to the resistive behaviour of R_{el} and $(R_{el} + R_p)$.

The observed localized process causes an increase in θ and decrease in Z at low frequencies [5, 25] (inductive behaviour). The medium frequency range is determined by the capacitance C and for a pure capacitive behaviour the slope of the $\log Z$ against $\log f$ curve should be -1 and θ rising towards $-90°$.

Figure 5 shows that the semicircles obtained are depressed, and the slopes of the $\log Z$ against $\log f$ curves are not -1. Deviations of this kind, often referred to as frequency dispersion, have been attributed to inhomogeneities of the solid surfaces.

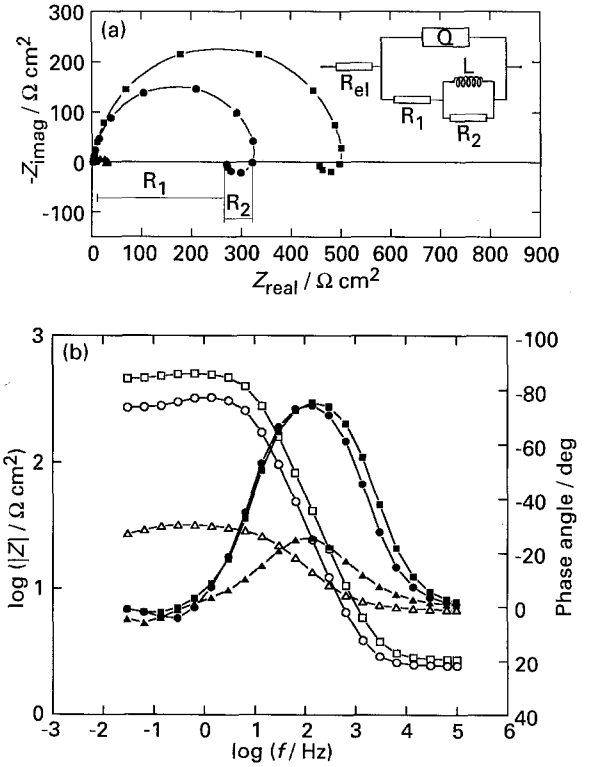

Fig. 5. (a) Nyquist plots for Al (●), AlMgSi (■) and AlZnMg electrode (▲) in 0.5 M NaCl solution, pH 1.3 at the open circuit potential. Equivalent circuit diagram for the total electrode impedance in detail. (b) Bode plots for Al (○, ●), AlMgSi (□, ■) and AlZnMg electrode (△, ▲) as in (a).

Table 2. Impedance parameters for Al, AlMgSi and AlZnMg electrodes at the open circuit potential in 0.5 M NaCl solution, pH 1.3

Parameters	*AlMgSi 0.5*	*Al 99.5*	*AlZn5Mg1*
$R_{el}/\Omega\,cm^2$	2.77	2.46	6.8
$Q/\mu F\,cm^{-2}$	44.17	72.79	883
n	0.930	0.935	0.700
$R_1/\Omega\,cm^2$	452	267	19.53
$R_2/\Omega\,cm^2$	55	68	6.51
$L/Hy\,cm^2$	57	30.28	14.15

A practical way to represent distributed processes such as corrosion of a rough and inhomogeneous electrode is with an element that follows its distribution. The constant phase element (CPE) meets that requirement. The impedance of CPE takes the form [33]:

$$Z_{CPE} = [Q(j\omega)^n]^{-1} \quad (6)$$

where the coefficient Q is a combination of properties related to both the surface and the electroactive species. The exponent n has values between -1 and 1. A value of -1 is characteristic of an inductance, a value of 1 corresponds to a capacitor, a value of 0 corresponds to a resistor and a value of 0.5 can be assigned to diffusion phenomena. For $n = 1$ and $n = -1$, the above equation becomes: $Z_c = (Cj\omega)^{-1}$ and $z_L = Lj\omega$, where L is the inductance.

The equivalent circuit used to fit the experimental data is presented as an insert in Fig. 5(a). This consists of CPE Q_1 ($n = 1$, $Q_1 = C$) in parallel to the series resistors R_1 and R_2 and a CPE Q_2 ($n = -1$, $Q_2 = L$) in parallel to R_2. R_{el} corresponds to the electrolyte resistance. The impedance corresponding to the equivalent circuit consisting of R_1, R_2, C and L may be considered a general term, including faradaic impedance effects. Characteristic values of Z_f are the charge transfer resistance, R_{ct}, and polarization resistance, R_p [34]. The charge transfer resistance corresponds to the sum of R_1 and R_2 and the polarization resistance to R_1. The capacity, C, is correlated to the thickness, d, and the dielectric constant, ϵ, of the barrier oxide film. Provided that there are no dielectric relaxations in the measurable frequency range, C can be expressed by $\epsilon\epsilon_0/d$, where ϵ is the dielectric constant, ϵ_0 the vacuum permittivity and d the layer thickness.

For each set of experimental data the parameters R_{el}, R_1, R_2, C and L were evaluated using a simple least square fit procedure and are presented in Table 2. The data were found to be sufficiently well fitted by the transfer function of the equivalent circuit presented in Fig. 5(a) within the limits of experimental error and reproducibility of data.

From Fig. 5 it can be seen that aluminium and AlMgSi samples show similar electrochemical behaviour in a 0.5 M NaCl solution, pH 1.3 although the polarization resistance of aluminium is somewhat reduced in comparison to that of AlMgSi alloy. The polarization resistance of AlZnMg alloy is drastically reduced in comparison with the other two samples, indicating that this alloy is exposed to severe corrosion in an acidic 0.5 M NaCl solution.

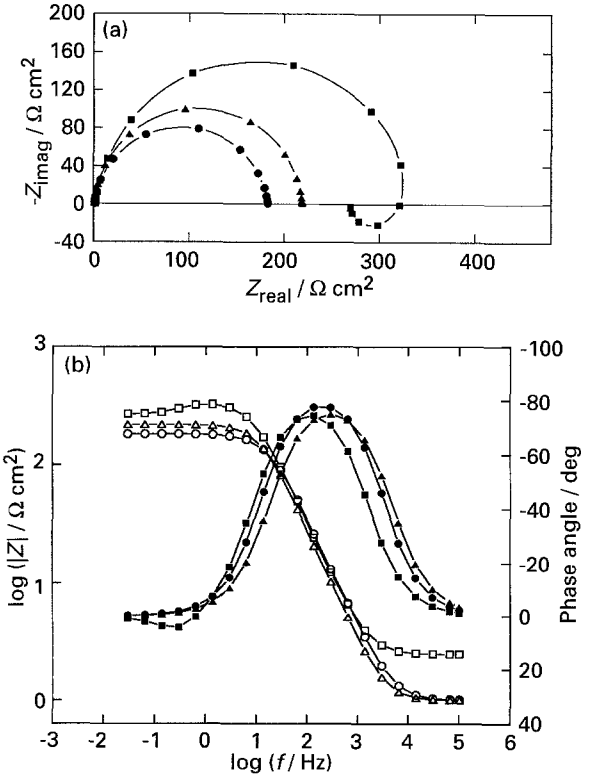

Fig. 6. (a) Nyquist plots for an aluminium electrode in 0.5 M NaCl solution, pH 1.3 at: (■) the open circuit potential (o.c.p.), (▲) −50 mV from o.c.p. and (○) −100 mV from o.c.p. (b) Bode plots for an aluminium electrode in 0.5 M NaCl solution, pH 1.3 at: (□, ■) the open circuit potential (o.c.p.), (△, ▲) −50 mV from o.c.p. and (○, ●) −100 mV from o.c.p.

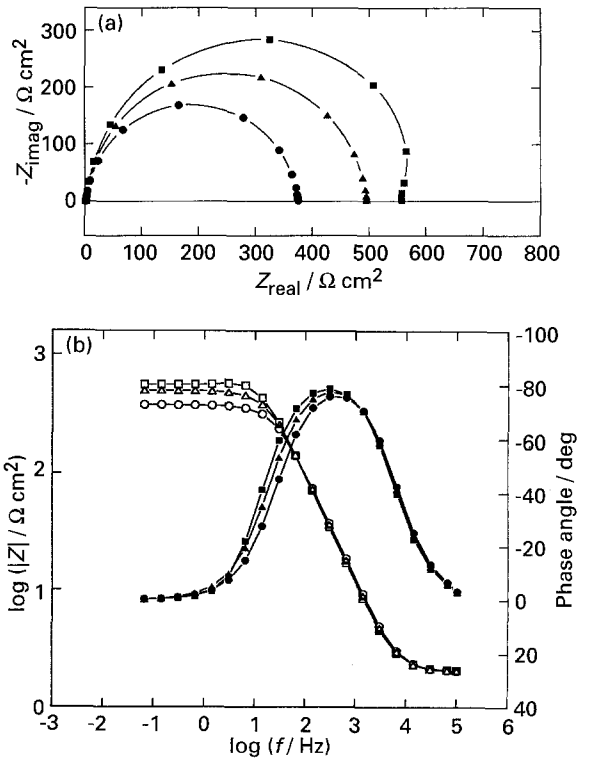

Fig. 7. (a) Nyquist plots for an aluminium electrode as in Fig. 6(a), but in the presence of 0.02 M triethanolamine. (b) Bode plots for an aluminium electrode as in Fig. 6(b).

Table 3. Impedance parameters for Al in 0.5 M NaCl solution, pH 1.3 at the open circuit potential and different electrode polarization

Parameters	*+50 mV*	*o.c.p*	*−50 mV*	*−100 mV*
$R_{el}/\Omega\,cm^2$	2.97	2.46	1	1
$Q/\mu F\,cm^{-2}$	2.70	72.79	75	70.5
n	0.970	0.935	0.952	0.925
$R_1/\Omega\,cm^2$	2.93	267	218	182
$R_2/\Omega\,cm^2$	37	68	–	–
$L/Hy\,cm^2$	8.2	30.28	–	–

Impedance measurements performed on cathodically polarized aluminium electrode in a 0.5 M NaCl solution, pH 1.3, presented in a form of Nyquist and Bode plots are shown, together with the measurements at open circuit potential, in Fig. 6(a) and (b). At higher cathodic polarization ($\geqslant 50$ mV) the low-frequency inductive loop has disappeared and the Nyquist plots exhibit only semicircular behaviour, indicating that the reaction is under charge transfer control. The observed R_{ct} value here represents the hydrogen evolution reaction on the oxide covered aluminium surface under the cathodic polarization, and it decreases with increasing cathodic polarization.

Impedance measurements performed as for Fig. 6, but in the presence of inhibitor at a concentration of 10^{-2} M are presented in Fig. 7(a) and (b). The addition of inhibitor in a 0.5 M NaCl solution, pH 1.3 has caused an increase in polarization resistance, indicating that the rate of the hydrogen evolution reaction has decreased. Figure 7 also shows that at o.c.p. the inductive loop has almost disappeared, suggesting that the localized corrosion has decreased in the presence of inhibitor. The values of R_{el}, R_1, R_2, C and L obtained for the aluminium electrode in a 0.5 M NaCl solution, pH 1.3 with and without addition of inhibitor at open circuit potential and different polarization are listed in Tables 3 and 4.

The results of impedance measurements show that the onset of pitting can be clearly determined by considering the low frequency range. It presents the inductive behaviour when pitting propagates and reaches an active state [5, 28].

4. Conclusions

The adsorption behaviour of triethanolamine on aluminium and AlMgSi and AlZnMg alloys covered with naturally formed oxide film was investigated in 0.5 M NaCl solution, pH 1.3 by means of potentiodynamic and electrochemical impedance spectroscopy techniques. The linear potential sweep technique with a sweep rate of $2\,mV\,s^{-1}$, and with a rotation rate of $2000\,min^{-1}$ was used. Impedance measurements were performed in the frequency range 30 mHz to 100 kHz.

The results of polarization measurements show that in all cases studied the addition of inhibitor induces a decrease in the cathodic currents without affecting the anodic polarization behaviour, and, accordingly, triethanolamine can be treated as a cathodic type inhibitor. The adsorption behaviour of triethanolamine on the electrode surface follows a Frumkin adsorption isotherm with constants: $a = 1.74$ and $B = 18.41\,dm^3\,mol^{-1}$.

The results of impedance measurements show a high frequency capacitive behaviour related to the dielectric properties of the oxide film and a low-frequency inductive part which was determined by the faradaic process and attributed to the localized corrosion. The $1/R_p$ values obtained from EIS measurements, as well as the corrosion currents obtained from polarization measurements, followed the sequence: AlMgSi < Al < AlZnMg.

With increasing cathodic polarization the low-frequency loop disappeared and only the capacitive loop was obtained, suggesting that the hydrogen evolution reaction on the oxide covered surface was under charge transfer control.

Table 4. Impedance parameters for Al in inhibited (0.02 M triethanolamine) 0.5 M NaCl solution, pH 1.3 at the open circuit potential (o.c.p.) and various cathodic polarization

Parameters	*o.c.p*	*−50*	*−100*
$R_{el}/\Omega\,cm^2$	2.08	2.04	2.04
$Q/\mu F\,cm^{-2}$	47.5	46.5	46.0
n	0.947	0.944	0.940
$R_1/\Omega\,cm^2$	555	494	373
$R_2/\Omega\,cm^2$	70	–	–
$L/Hy\,cm^2$	7	–	–

References

[1] M. Pourbaix, 'Atlas of Electrochemical Equilibria in Aqueous Solutions', National Association of Corrosion Engineers, Houston (1974) p. 168.
[2] C. M. A. Brett, *J. Appl. Electrochem.* **20** (1990) 1000.
[3] S. E. Frers, M. M. Stefanel, C. Mayer and T. Chierchie, *ibid.* **20** (1990) 996.
[4] J. Bessone, C. Mayer, K. Jüttner and W. J. Lorenz, *Electrochim. Acta* **28** (1983) 171.
[5] J. B. Bessone, D. R. Salinas, C. E. Mayer, M. Ebert and W. J. Lorenz, *ibid.* **37** (1992) 2283.
[6] F. D. Bogar and R. T. Foley, *J. Electrochem. Soc.* **119** (1972) 462.
[7] W. M. Moore, C. T. Chen and G. A. Shirn, *Corrosion* **40** (1984) 644.
[8] T. R. Beck, *Electrochim. Acta* **33** (1988) 1321.
[9] L. Tomcsanyi, K. Varga, I. Bartik, G. Horanyi and E. Maleczki, *ibid.* **34** (1989) 855.
[10] S. Szklarska-Smialowska, *Corros. Sci.* **33** (1992) 1193.
[11] C. Brett, *ibid.* **33** (1992) 203.
[12] Z. Sklarska-Smialowska, 'Pitting Corrosion of Metals', NACE, Houston, Texas (1986) p. 296.
[13] G. Schmitt, *Br. Corros. J.* **19** (1984) 166.
[14] T. M. Salem, J. Horvath and P. S. Sidky, *Corros. Sci.* **18** (1978) 363.
[15] J. D. Talati and D. K. Gandi, *ibid.* **23** (1983) 1315.
[16] M. S. Abdel-Aal, M. Th. Makhlot and A. A. Hermas, Proceedings of the 7th European Symposium on Corrosion Inhibitors, Ann. Univ. Ferrara, N.S., Sez. V, Suppl. N. 9 (1990) p. 1143.
[17] G. Trabanelli, *in* 'Corrosion Mechanisms', (edited by F. Mansfeld), Marcel Dekker, New York (1987) p. 119.
[18] S. Trasatti, *Electrochim. Acta* **37** (1992) 2137.
[19] I. L. Rozenfeld, 'Corrosion Inhibitors', MacGraw-Hill, New York (1981).
[20] L. A. Avaca, E. R. Gonzalez and A. R. Filho, *J. Appl. Electrochem.* **12** (1982) 405.
[21] K. Jüttner, *Electrochim. Acta* **35** (1990) 1501.

[22] F. Mansfeld, *ibid.* **35** (1990) 1533.
[23] J. Hitzig, K. Jüttner, W. J. Lorenz and W. Paatasch, *J. Electrochem. Soc.* **133** (1986) 887.
[24] F. Mansfeld and M. W. Kendig, *ibid.* **135** (1988) 829.
[25] F. Mansfeld, S. Lin, S. Kim and H. Shih, *Werkst. Korros.* **39** (1988) 487.
[26] C. Monticelli, G. Brunoro, A. Frignani and F. Zucchi, *Corros. Sci.* **32** (1991) 693.
[27] C. Monticelli, G. Brunoro and G. Trabanelli, Proceedings of the 7th European Symposium on Corrosion Inhibitors, Ann. Univ. Ferrara, N.S., Sez. V, Suppl. N. 9 (1990) p. 1125.
[28] M. J. Dignam, *in* 'Oxides and Oxide Films', (edited by J. W. Diggle), Vol. 1, Marcel Dekker, New York (1972) p. 91.
[29] K. Kobayashi and K. Ishil, Proceedings of the 5th European Symposium on Corrosion Inhibitors, Vol. 2, Ferrara (1980).
[30] J. J. de Damborenea and A. J. Vazquez, Proceedings of the 7th European Symposium on Corrosion Inhibitors, Ann. Univ. Ferrara, N.S., Sez. V. Suppl. N. 9 (1990) p. 137.
[31] A. N. Frumkin and B. Damaskin, *in* 'Modern Aspects of Electrochemistry', (edited by J. O'M. Bockris and B. E. Conway), Vol. 3. Butterworths, London (1964).
[32] J. O'M. Bockris and D. A. J. Swinkels, *J. Electrochem. Soc.* **111** (1964) 736.
[33] W. J. Lorentz and F. Mansfeld, *Corros. Sci.* **21** (1981) 647.
[34] J. R. Macdonald, *J. Electroanal. Chem.* **223** (1987) 25.